Cortical thinning pattern according to differential nigrosome involvement in patients with Parkinson's disease

Na-Young Shin[a], Bo-Hyun Kim[b], Eunkyeong Yun[c], Uicheul Yoon[c], Jong-Min Lee[b], Young Hee Sung[d], Eung Yeop Kim[e],*

[a] Department of Radiology, Seoul St. Mary's Hospital, College of Medicine, The Catholic University of Korea, Seoul 06591, Republic of Korea
[b] Department of Biomedical Engineering, Hanyang University, Seoul 04763, Republic of Korea
[c] Department of Biomedical Engineering, College of Bio and Medical Sciences, Daegu Catholic University, Gyeongbuk 38430, Republic of Korea
[d] Department of Neurology, Gil Medical Center, Gachon University College of Medicine, Incheon 21565, Republic of Korea
[e] Department of Radiology, Gil Medical Center, Gachon University College of Medicine, Incheon 21565, Republic of Korea

ARTICLE INFO

ABSTRACT

The pathological hallmark of Parkinson's disease (PD) is the progressive degeneration of dopaminergic neurons in the substantia nigra pars compacta, where the dopaminergic neurons form five clusters called nigrosomes 1–5 (N1–N5). N1 is the largest and considered to be the most affected by PD, followed by N2, N4, N3, and N5. Recently, an MRI study suggested a sequential progression of loss from N1 to N4. As the extent of cortical thinning widens as PD progresses, we aimed to define cortical thinning patterns according to the differential involvement of N1 and N4 in PD patients. Cortical thickness was analyzed in 83 PD patients (29 with N1 loss on at least one side of the brain, but no N4 loss; and 54 with N4 loss on at least one side) and 35 healthy subjects with age, sex, disease duration, and intracranial volume as covariates. On patient-wise analysis, for areas with more cortical thinning than the controls, PD patients with N4 loss had wider cortical thinning involving more dorsolateral prefrontal cortex and temporal areas than PD patients with only N1 loss, but cortical thinning did not significantly differ between these two patient groups. However, cortical thinning was more apparent in hemisphere-level analysis with statistically significant clusters being found more in hemispheres with N4 loss than hemispheres with N1 loss in PD patients compared to normal hemispheres of the controls. Cortical thinning occurred in a similar propagation pattern to that seen with PD progression, supporting past hypotheses on the sequential progression of nigrosome loss from N1 to N4.

1. Introduction

The pathological hallmark of Parkinson's disease (PD) is the progressive degeneration of dopaminergic neurons in the substantia nigra pars compacta (SNc). The dopaminergic neurons within the SNc form five clusters called nigrosomes 1–5 (N1–N5). Among these clusters, N1 is the largest and is considered to be the most affected by PD, followed by N2, N4, N3, and N5 (Damier et al., 1999a, 1999b). As cell loss in N1 has been found even in PD patients with shorter disease duration and cell loss in N2, N4, N3, and N5 has been found in patients with longer disease duration with loss progressing in the sequential order given above, the authors of this past study suggested that there was a stereotyped temporospatial progression pattern in dopaminergic cell loss within SNc (Damier et al., 1999b). However, with only five brains being

included as study subjects, the findings of this study could only be considered as a hypothesis rather than a conclusive observation.

Thanks to its large size, N1 is visible as a hyperintense structure in the posterior region of SNc on T2* or susceptibility-weighted imaging (SWI) not only on ultra-high-field MRI (Blazejewska et al., 2013; Cosottini et al., 2014; Kwon et al., 2012) but also on widely available 3T MRI (Noh et al., 2015; Schwarz et al., 2014; Sung et al., 2016). Also, N1 loss is now considered an imaging biomarker for degenerative parkinsonism (Mahlknecht et al., 2017). However, imaging findings of nigrosome subregions other than N1 have scarcely been reported. In a previous ex-vivo study, 9.4T MRI delineated all nigrosome subregions (Massey et al., 2017). In an in-vivo study using 3T MRI, only putative N4 regions were observed as hyperintense structures located in the medial half of posterior SN at the lower one-third level of the red

---

nucleus (Sung et al., 2018). In this study, the authors reported that loss of normal hyperintensity in both N1 and N4 occurred more frequently in late-stage PD, while N1 loss without accompanying N4 loss was more frequently observed in early-stage PD. Moreover, N4 loss always followed N1 loss, supporting a sequential progression of loss from N1 to N4 (Sung et al., 2018). The sequential progression of nigrosome loss may be further supported by finding wider abnormalities in other brain regions of patients with N4 loss than those with N1 loss.

Cortical thinning is found in the orbitofrontal gyrus, anterior cingulate gyrus, postcentral gyrus, and some temporal, parietal, and occipital areas even in early-stage PD (Uribe et al., 2018) and the extent of the involved region widens to the medial and lateral prefrontal, temporal, and parietal cortices as PD progresses (Yau et al., 2018; Zarei et al., 2013). If a wider cortical thinning area is observed with N4 loss compared to N1 loss in a pattern similar to previously reported propagation patterns for cortical thinning, it would support the sequential involvement of nigrosomes from N1 to N4. Knowledge on additional cortical thinning areas relevant to N4 loss might help us build up a comprehensive clinical picture of N4 loss. We therefore aimed to define whether differential involvement of N1 and N4 may affect the degree of cortical thinning in patients with PD.

2. Materials and methods

2.1. Subjects

This retrospective study was approved by the Institutional Review Board and a waiver of informed consent was obtained for the review of patient images and medical records.

Patients were recruited from the database of a movement disorder clinic in a single tertiary hospital. From November 2014 to March 2017, 91 consecutive patients with PD who underwent MRI including a nigrosome imaging protocol were selected. PD was diagnosed with the clinical diagnostic criteria of the United Kingdom Parkinson's Disease Society Brain Bank (Hughes et al., 1992). Motor symptoms were assessed with the Hoehn and Yahr (H&Y) scales (Hoehn and Yahr, 1967) and Unified Parkinson's Disease Rating Scale, Part III (UPDRS III). General cognitive function was assessed with the Korean version of the Mini-Mental State Examination (Folstein et al., 1975). We only included patients with decreased dopamine transporter uptake in either side of the posterior putamen on N-3-fluoro- propyl-2-b-carbomethoxy-3-b-(4-iodophenyl) nortropane PET (FP-CIT PET) observed with a PET/CT scanner (Biograph-6; Siemens) to ensure clinical diagnostic accuracy. To reduce the effect of other conditions besides PD on cortical thickness, patients with tumors, hemorrhage, infarcts, and severe white matter hyperintensities on MRI and those with other neurodegenerative diseases and medical comorbidities that might account for cognitive dysfunction were excluded.

Thirty-seven age- and sex-matched healthy controls (HC) without history of neurologic or psychiatric disease, family history of movement disorders, and symptoms or signs indicative of prodromal PD were also recruited.

2.2. Image acquisition

All participants underwent 3T MRI with a 32-channel head coil (MAGNETOM Skyra; Siemens Healthineers, Forchheim, Germany).

To assess N1 and N4, oblique coronal 3D multi-echo combination imaging (MEDIC), which was used to generate susceptibility map-weighted imaging (SMWI) images (Nam et al., 2017), was obtained parallel to the plane from the posterior commissure to the top of the pons with the following parameters: TR = 88 ms; minimum TE = 11.1 ms; maximum TE = 66.9 ms; six echoes; echo spacing = 11.1 ms; flip angle = 108; echo train length = 6; thickness = 1 mm; number of sections = 28; matrix = 384 × 384; FOV = 192 × 192; voxel size = 0.5 × 0.5 × 1.0 mm^3; acceleration
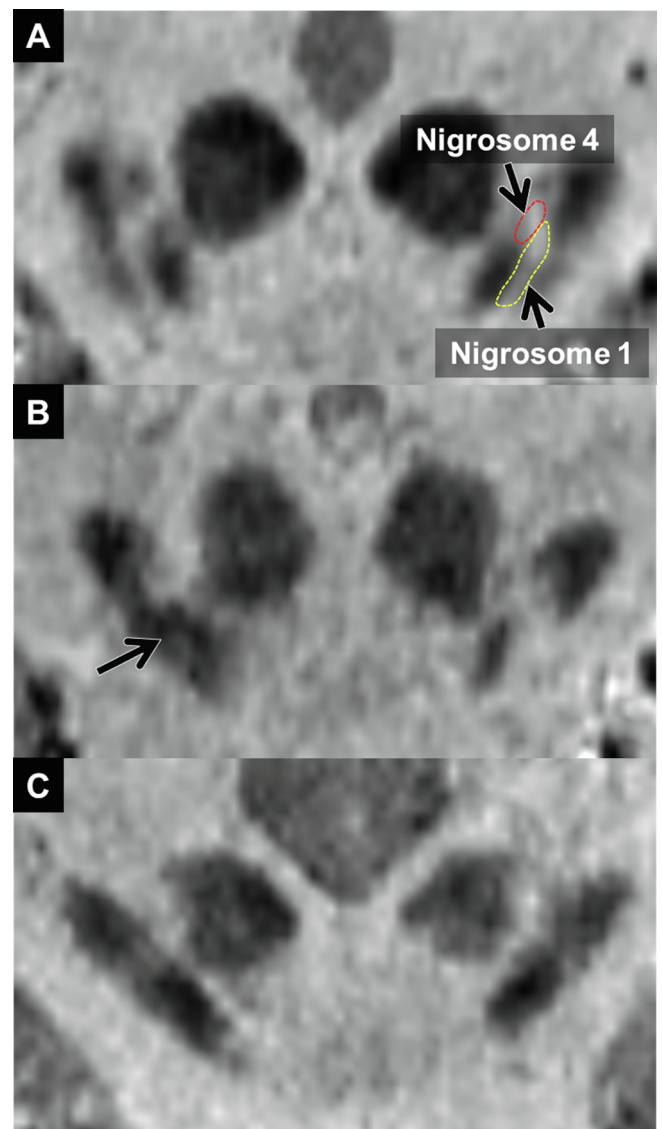
Fig. 1. Representative reformatted images of normal and abnormal N1 and N4. A. A 62-year-old healthy female showed normal nigrosome 1 and 4 on both sides. B. A 57-year-old female with early-stage PD (H&Y 1) showed loss of nigrosome 1 on the right side (arrow). C. A 78-year-old male with late-stage PD (H&Y 4) showed loss of nigrosome 1 and 4 on both sides.

factor = 2; and acquisition time = 7 min 19 s.

For cortical thickness analysis, whole-brain sagittal 3D magnetization-prepared rapid acquisition gradient echo (MPRAGE) imaging was obtained with the following parameters: TR = 1800 ms; TE = 3 ms; TI = 920 ms; matrix = 256 × 256; FOV = 250 × 250; voxel size = 1.0 × 1.0 × 1.0 mm^3; acceleration factor = 2; and acquisition time = 3 min 36 s.

2.3. Analysis of nigrosomes

N1 and N4 were evaluated on oblique coronal SMWI images reformatted perpendicular to the midbrain axis with an increment of 0.2 mm. As described in a previous study (Sung et al., 2018), N1 was defined as the central hyperintense region between two hypointense layers in the posterior substantia nigra at the level below the red nucleus. N4 was defined as the hyperintense region located in the medial half of the substantia nigra at the lower one-third level of the red nucleus. A neuroradiologist and a neurologist evaluated the integrity of hyperintensity for both N1 and N4 in each hemisphere. If
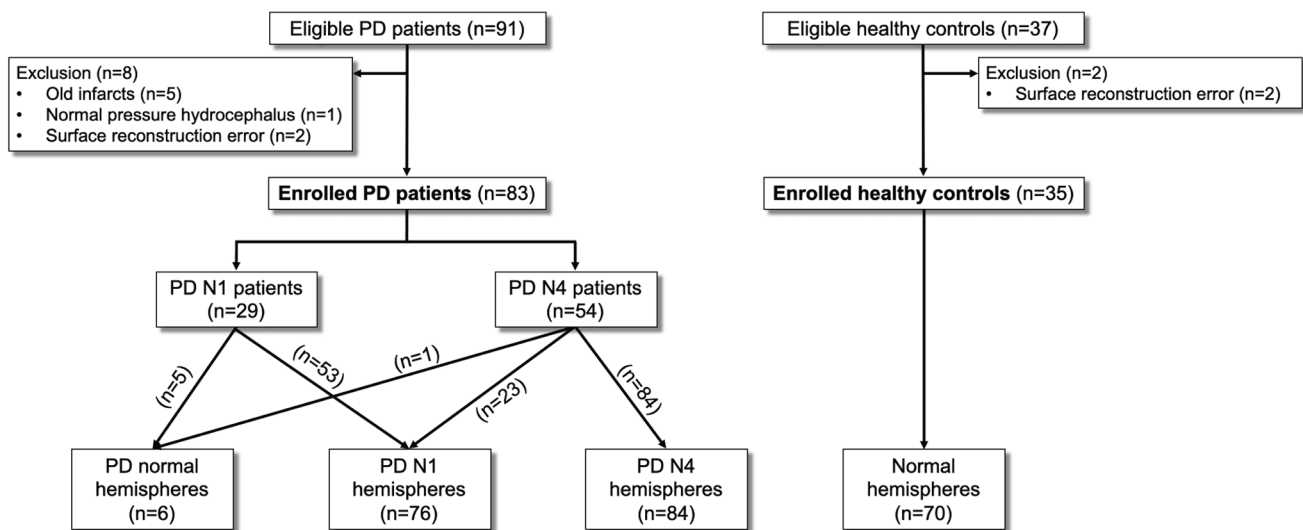
Fig. 2. Flowchart of the study subjects.

hyperintensity was replaced by hypointensity, the corresponding nigrosome was thought to be lost (Fig. 1).

For patient-level analysis, we divided the subjects into three groups: the HC group, the PD N1 group for PD patients with N1 loss found on either side of the brain, but with intact N4 on both sides of the brain, and the PD N4 group for PD patients with N4 loss found on either side of the brain.

For hemisphere-level analysis, we divided the cerebral hemispheres into four types: normal hemispheres for the controls, PD normal hemispheres for the hemispheres of PD patients with intact N1 and N4, PD N1 hemispheres for the hemispheres of PD patients with N1 loss but intact N4, and PD N4 hemispheres for the hemispheres of PD patients with both N1 and N4 loss.

2.4. Cortical thickness analysis

For patient-level analysis, we used the CIVET pipeline (http://mcin.ca/civet/) to measure cortical thickness, as was described in detail elsewhere (Shin et al., 2017, 2016). Each subject's native T1-weighted images were corrected for intensity inhomogeneity and spatially normalized to the MNI-152 symmetric template (Collins et al., 1994; Sled et al., 1998). After that, tissue classification was performed (Zijdenbos et al., 2002) and hemispheric inner and outer cortical surfaces were automatically extracted using the constrained Laplacian-based automated segmentation with the proximities algorithm (Kim et al., 2005; McDonald et al., 2006). Cortical thickness was measured by calculating the Euclidean distance between corresponding vertices on the grey matter/cerebrospinal fluid intersection surface and the white matter/gray matter boundary surface (Kabani et al., 2001; Lerch and Evans, 2005; McDonald et al., 2006). Diffusion smoothing with a 20-mm full width at half maximum kernel (FWHM) was used to increase the signal-to-noise ratio.

For hemisphere-level analysis, all T1-weighted images were processed with the same pipeline used in the patient-level analysis. The cortical thickness of 40,962 vertices on the right hemisphere was mapped to the corresponding vertices on the left hemisphere. Thus, the number of hemispheres included in the hemisphere-level analysis was twice that of the patients included in the patient-level analysis.

For both patient-level and hemisphere-level analyses, cortical thickness was compared between each group pair at each vertex using ANCOVA with age, sex, disease duration, and intracranial volume entered as covariates. Disease duration was defined as time interval in months from the development of motor symptoms due to PD to the time of MRI examination, and was considered to be zero for control subjects.

We used SurfStat (http://www.math.mcgill.ca/keith/surfstat/) for the vertex-wise analysis with the random field theory and a false discovery rate threshold of $P < 0.05$ to control for multiple comparisons.

2.5. Statistical analysis

Clinical characteristics were compared between the three groups. According to the test results for normal distribution, continuous variables were presented as mean ± standard deviation (SD) or median (interquartile range) and compared with ANOVA or the Kruskal-Wallis test, respectively. Categorical variables were compared with the Chi-square or Fisher's exact test as appropriate. To examine pair-wise differences between the groups, post-hoc analyses were also performed with the Bonferroni-corrected Student's t-test, Wilcoxon rank-sum test, Chi-square test, or Fisher's exact test as appropriate. To compare PD stage, H&Y scale, disease duration, UPDRS III and MMSE score between the PD N1 and PD N4 groups, the Chi-square test, Fisher's exact test, and the Wilcoxon rank-sum test were performed, respectively. A P value of < 0.05 was considered statistically significant. Statistical analyses were conducted using R Statistical Software (version 3.5.1; R Foundation for Statistical Computing, Vienna, Austria).

3. Results

3.1. Clinical characteristics

Among 91 PD patients, five had old infarcts, one had normal pressure hydrocephalus, and two had errors occur during surface reconstruction of their structural MRI. Two of the 37 control subjects also had surface reconstruction errors. After excluding these patients, 83 PD patients and 35 controls were finally included in this study. Twenty-nine patients showed N1 loss (both sides [n = 24]; only left side [n = 4]; and only right side [n = 1]) without N4 loss. Fifty-four patients showed N4 loss (both sides [n = 30]; only left side [n = 13]; and only right side [n = 11]). All patients with N4 loss had bilateral N1 loss with the exception of one patient who had ipsilateral N1 loss. Therefore, there were 70 normal hemispheres, 6 PD normal hemispheres, 76 PD N1 hemispheres, and 84 PD N4 hemispheres (Fig. 2).

There was no significant difference in age and sex between the three groups. The PD N4 group had more late-stage PD patients with higher H&Y scales and UPDRS III scores, but no significant difference in disease duration compared to the PD N1 group. Twelve (42.9%) of the 29 patients in the PD N1 group and 29 (54.7%) of 54 patients in the PD N4 group had scores below 25—the suggested diagnostic cut-off point for

Table 1
Demographic and clinical characteristics.

Group	HC (n = 35)	PD N1 (n = 29)	PD N4 (n = 54)	P value
Age	68.00 [65.00–71.00]	71.00 [58.00–76.00]	73.00 [67.00–77.00]	0.062
Sex				0.061
Male	11 (31.43%)	11 (37.93%)	30 (55.56%)	
Female	24 (68.57%)	18 (62.07%)	24 (44.44%)	
PD stage				0.002
Early stage (H&Y ≤ 2)	–	25 (86.21%)	26 (48.15%)	
Late stage (H&Y > 2)	–	4 (13.79%)	28 (51.85%)	
H&Y scale				0.015
(1/1.5/2/2.5/3/4/5)	–	9/1/15/1/3/0/0	7/0/19/11/11/5/1	
Disease duration, m		9.00 [4.00–18.00]	16.00 [6.00–34.00]	0.063
UPDRS III	–	15.00 [3.00–20.00]	22.00 [15.00–29.00]	0.027
MMSE	–	25.00 [22.00–28.00]	23.50 [18.75–23.25]	0.388
Score < 25		12 (42.9%)	29 (54.7%)	0.434

Data are medians [interquartile ranges] or numbers (percentages).

detecting dementia in PD patients (Folstein et al., 1975)—on MMSE. No significant differences in MMSE scores and the number of patients with MMSE scores below 25 were found between the groups. Although MMSE cannot diagnose dementia alone (Kim et al., 2016; Mitchell, 2009), some patients in both groups of our cohort are likely to have dementia (Table 1).

3.2. Patient-level cortical thickness analysis

Compared to the controls, the PD N1 group showed thinning in the bilateral orbitofrontal cortex, bilateral dorsolateral prefrontal cortex, bilateral medial prefrontal cortex, and some areas of the temporal cortex. Cortical thinning worsened and widened to the bilateral frontal, parietal, and temporal areas in the PD N4 group relative to the controls (Fig. 3). However, there were no statistically significant differences in cortical thickness between groups after multiple comparison correction.

### 3.3. Hemisphere-level cortical thickness analysis

Compared to the normal hemispheres of the controls, the normal hemispheres of PD patients had significantly increased cortical thickness in the medial and lateral occipital gyri. Compared to the normal hemispheres of the controls, the PD N1 hemispheres showed significant cortical thinning in the primary sensory/motor cortex, orbitofrontal cortex, medial and lateral prefrontal cortex, precuneus/posterior cingulate gyrus, and superior temporal gyrus. The PD N4 hemispheres showed similar patterns of cortical thinning with the PD N1

hemispheres, but additional cortical thinning areas were found in the superior and middle frontal gyri, superior, middle, and inferior temporal areas, and supramarginal and angular gyri (Fig. 4). Compared with the normal hemispheres of PD patients, the PD N1 hemispheres showed significant cortical thinning in the medial and lateral occipital gyri, while no significant difference was found in the PD N4 hemispheres. Also, no significant clusters differed between the PD N1 and PD N4 hemispheres (Table 2).

4. Discussion

In this study, we found a distinct pattern of cortical thinning according to the differential involvement of N1 and N4. On patient-wise analysis, for areas in which patients showed more cortical thinning compared to the controls, PD patients with N4 loss had wider cortical thinning that involved more dorsolateral prefrontal cortex and temporal areas than patients with only N1 loss. This change was more apparent in the hemisphere-level analysis with statistically significant clusters being found more in the PD N4 hemispheres than the PD N1 hemispheres compared to the normal hemispheres of the controls. This cortical thinning pattern was similar to the cortical thinning propagation previously seen with PD progression (Yau et al., 2018; Zarei et al., 2013), supporting the hypothesis of sequential progression of loss from N1 to N4.

The topographical organization of nigrostriatal fibers and striato-cortical fibers has been well described in both animals and humans (Beckstead et al., 1979; Draganski et al., 2008; Lehéricy et al., 2004;
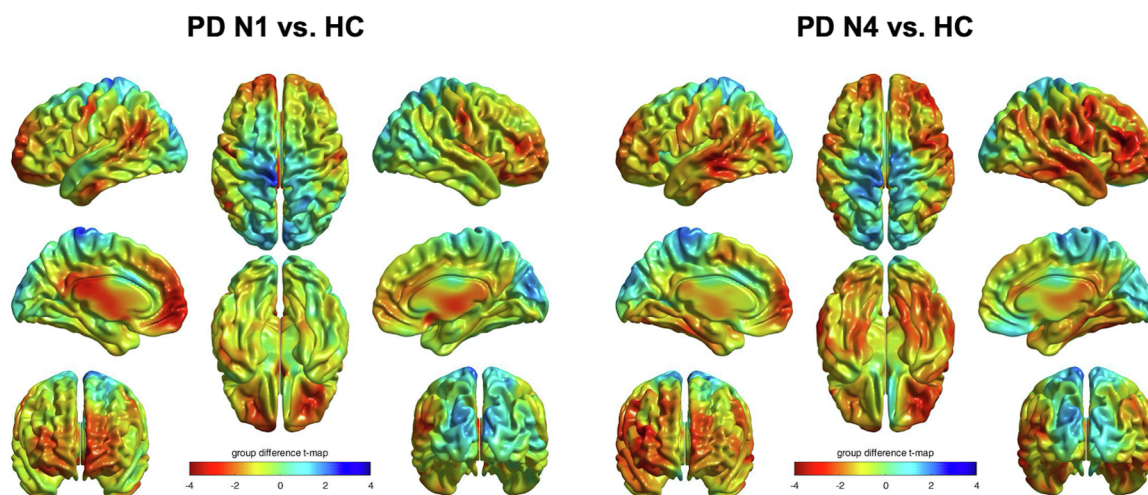
Fig. 3. Patient-level group differences for cortical thickness. Color maps show *t*-statistics comparing the PD N1 and N4 groups to the healthy control (HC) group at each cortical vertex. Warm colors indicate cortical thinning and cool colors indicate cortical thickening in the PD N1 and N4 groups compared to the HC group.
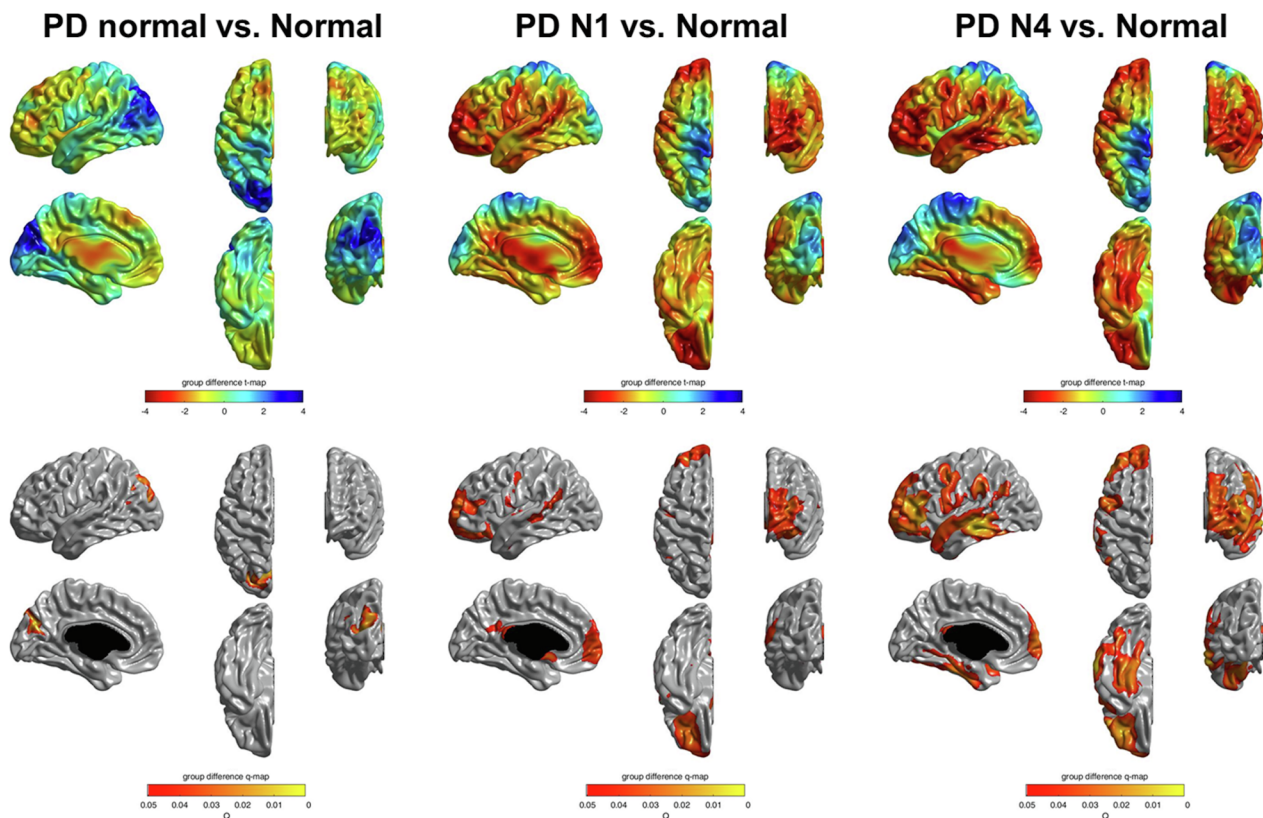
Fig. 4. Hemisphere-level group differences in cortical thickness. Color maps show *t*-statistics that compare each group pair in the upper panel. Threshold maps show areas of significant difference after multiple comparison corrections (false discovery rate-corrected $p < 0.05$) in the lower panel.

Lenglet et al., 2012; Marquand et al., 2017). Posterolateral parts of SNc (e.g., N1) project to the posterolateral regions of the striatum, and the more anteromedial parts of SNc (e.g., N4) project to the anteromedial regions of the striatum (Beckstead et al., 1979; Lenglet et al., 2012). Subsequently, the posterolateral putamen connects to the cortical regions related to motor function; the dorsal and posterior caudate connects to the ventrolateral prefrontal cortex, angular gyrus, and posterior temporal area; the more anteromedial striatum connects to the dorsolateral prefrontal cortex, insula, and anterior temporal area; and the most ventromedial and anterior part of striatum connects to the ventromedial prefrontal cortex and other limbic areas such as the amygdala and hippocampus (Marquand et al., 2017). Given that dopaminergic neuronal loss occurs unevenly and possibly starts from the ventrolateral part of SNc in PD (Damier et al., 1999b), as reflected in the posterior to

anterior gradient of decreased uptake in the striatum on dopamine transporter imaging (Nandhagopal et al., 2009), we may postulate that cortical thinning starts from the motor cortex to the ventrolateral prefrontal cortex, temporoparietal junction, and some temporal areas, and then to the dorsolateral prefrontal cortex and limbic areas as PD progresses. In line with this assumption, our results showed cortical thinning in the motor cortex, ventrolateral prefrontal cortex, and supramarginal/angular gyri in the less affected PD N1 hemispheres with additional cortical thinning in the dorsolateral prefrontal cortex and temporal area in the more affected PD N4 hemispheres. This pattern is also concordant with previous cross-sectional (Zarei et al., 2013) and longitudinal studies (Yau et al., 2018) which showed the propagation of cortical thinning as disease progressed.

It is noteworthy that the ventromedial prefrontal cortex and

Table 2
Regions of significant cortical thinning with multiple comparison corrections based on the false discovery rate in hemisphere-level analysis.

	No. of vertex	Cluster-wise p	Vertex-wise t	Vertex-wise p	x	y	z	AAL region
PD normal > Normal	833	0.009	4.487	0.005	−7.55	−72.36	24.80	Superior occipital gyrus
	26	0.018	3.698	0.076	−41.05	−67.60	33.25	Middle occipital gyrus
Normal > PD N1	2825	0.027	3.568	0.115	−36.43	43.05	−11.46	Middle frontal gyrus, orbital part
	706	0.033	3.282	0.267	−51.27	−45.03	21.11	Superior temporal gyrus
	188	0.037	3.068	0.479	−50.30	−9.50	46.57	Precentral gyrus
	152	0.037	3.069	0.477	−0.62	−36.98	23.41	Precuneus
	62	0.040	2.828	0.871	−57.54	−1.34	13.62	Postcentral gyrus
Normal > PD N4	4085	0.007	4.162	0.016	−60.88	−34.29	−3.78	Middle occipital gyrus
	3667	0.011	3.900	0.039	−36.69	39.13	12.74	Middle temporal gyrus
	1205	0.021	3.244	0.297	−45.78	3.52	46.94	Precentral gyrus
	448	0.022	3.186	0.349	−58.20	−32.84	34.20	Supramarginal gyrus
	405	0.024	3.043	0.510	−46.24	−59.14	31.14	Angular gyrus
	47	0.031	2.773	0.991	−0.84	−39.09	21.81	Precuneus
PD normal > PD N1	813	0.002	5.022	< 0.001	−9.14	−71.91	24.00	Cuneus
	101	0.018	3.789	0.057	−41.98	−65.04	17.01	Middle occipital gyrus
	87	0.006	4.288	0.010	−41.05	−67.60	33.25	Middle occipital gyrus

precuneus/posterior cingulate cortex showed cortical thinning in the PD N1 hemisphere, even though these areas are known to be connected to the most ventromedial and anterior part of the striatum, which is generally the last involved area in PD. As these areas are also associated with olfaction (Zhou et al., 2019), early pathologic involvement of the olfactory bulb (Braak et al., 2003) along with cortical thinning in associated areas may be responsible for the above findings. These areas also overlap with the default mode network where patients with Alzheimer's disease showed decreased functional connectivity in resting state (Greicius et al., 2004) and cortical atrophy (Du et al., 2006; Lee et al., 2018). The relatively frequent presence of Alzheimer-type pathology in PD patients (Mastaglia et al., 2003), and subsequent Alzheimer-pattern cortical atrophy might account for our results.

Unexpectedly, increased cortical thickness in the medial and lateral occipital gyri was found in the PD normal hemispheres compared to normal and PD N1 hemispheres. The significant occipital cortical thickening disappeared in the PD N1 and PD N4 hemispheres. Although this result should be interpreted cautiously due to the small number of PD normal hemispheres (n = 6) assessed, a previous study also reported cortical thickening in the medial occipital gyrus in early untreated PD patients (Uribe et al., 2018). In this previous study, among two patterns of cortical atrophy, one that was mainly affected in the anterior brain areas showed cortical thickening in the occipital gyrus without detectable cognitive impairment. Meanwhile, the other pattern with predominant atrophy in the posterior brain area (Uribe et al., 2018), including the occipital cortex, showed worse cognitive and motor performance. The authors suggested neuroinflammation as a possible cause for the occipital cortical thickening. A previous study using free-water imaging (Andica et al., 2019) reported that an imaging marker of neuroinflammation was predominant in the posterior brain areas, while that of neurodegeneration was predominant in the anterior brain areas in early-stage PD patients. These findings support the sequence of neuroinflammation followed by neurodegeneration. Accordingly, occipital cortical thickening might be a transient phenomenon in the early stages of PD, and as the disease progresses, occipital cortical thickness might decrease and become atrophic. Other previous studies have also reported preserved occipital cortical thickness in PD patients with normal cognition or moderate stage, but occipital cortical thickness decreases in those with cognitive impairment or advanced stage (Baggio et al., 2015; Pereira et al., 2014).

As N4 loss was associated with cortical thinning in the dorsolateral prefrontal cortex and temporal areas, we expected patients with N4 loss to have lower cognitive function than those with N1 loss. However, there was no significant difference in MMSE scores between the two groups. More detailed neuropsychological assessments might be able to capture subtle changes in various cognitive domains. Also, further studies that assess non-motor symptoms in more detail might help define the clinical implications of the differential involvement of nigrosomes.

Our study has several limitations. First, this study is a cross-sectional study which is limited to investigating the sequential changes in brain atrophy with disease progression. Although a recent study (Schwarz et al., 2018) has also reported graded T2*-weighted signal alterations in nigrosomes and surrounding iron-rich SN in PD, which further supports previous pathologic studies on the sequential involvement of nigrosomes, (Damier et al., 1999b), longitudinal studies are still necessary to elucidate the sequential involvement of nigrosomes in pre-mortem PD patients at an individual level. Second, as aforementioned, we did not perform extensive neuropsychological assessments on PD patients, and therefore, their cognitive status could not be determined which limits how much we can understand about the clinical impact of differential N1 and N4 loss. Lastly, there might be other factors which we did not control for that might affect cortical thinning. Longitudinal studies with intra-individual comparisons according to different time points might help overcome this issue.

5. Conclusion

Our results showed wider cortical thinning in PD patients with N4 loss than those with N1 loss compared to the controls. The pattern of cortical thinning was similar to the propagation of cortical thinning seen with PD progression, supporting the hypothesis of sequential progression of nigrosome loss from N1 to N4. However, only longitudinal studies can draw definitive conclusions. Moreover, cortical thickness was not significantly different when the PD N1 group was directly compared to the PD N4 group. Further studies using other imaging markers (e.g., diffusion tensor imaging) which can detect brain alterations in PD patients with more sensitivity might also help unveil the effect of differential involvement of nigrosomes.

CRediT authorship contribution statement

Na-Young Shin: Conceptualization, Formal analysis, Funding acquisition, Investigation, Methodology, Writing - original draft. **Bo-Hyun Kim:** Formal analysis, Visualization. **Eunkyeong Yun:** Formal analysis, Visualization. **Uicheul Yoon:** Formal analysis, Visualization. **Jong-Min Lee:** Formal analysis, Visualization. **Young Hee Sung:** Data curation, Funding acquisition. **Eung Yeop Kim:** Data curation, Conceptualization, Methodology, Supervision, Writing - review & editing.

Declaration of Competing Interest

The authors declare that they have no known competing financial interests or personal relationships that could have appeared to influence the work reported in this paper.

References

Andica, Kamagata, Hatano, Saito, Uchida, Ogawa, Takeshige-Amano, Zalesky, Wada, Suzuki, Hagiwara, Irie, Hori, Kumamaru, Oyama, Shimo, Umemura, Pantelis, Hattori, Aoki, 2019. Free-water imaging in white and gray matter in Parkinson's disease. Cells 8, 839. https://doi.org/10.3390/cells8080839.

Baggio, H.-C., Segura, B., Sala-Llonch, R., Marti, M.-J., Valldeoriola, F., Compta, Y., Tolosa, E., Junqué, C., 2015. Cognitive impairment and resting-state network connectivity in Parkinson's disease: connectivity in Parkinson's Disease. Hum. Brain Mapp. 36 (1), 199–212.

Beckstead, R.M., Domesick, V.B., Nauta, W.J.H., 1979. Efferent connections of the substantia nigra and ventral tegmental area in the rat. Brain Res. 175 (2), 191–217.

Blazejewska, A.I., Schwarz, S.T., Pitiot, A., Stephenson, M.C., Lowe, J., Bajaj, N., Bowtell, R.W., Auer, D.P., Gowland, P.A., 2013. Visualization of nigrosome 1 and its loss in PD: pathoanatomical correlation and in vivo 7 T MRI. Neurology 81 (6), 534–540.

Braak, H., Tredici, K.D., Rüb, U., de Vos, R.A.I., Jansen Steur, E.N.H., Braak, E., 2003. Staging of brain pathology related to sporadic Parkinson's disease. Neurobiol. Aging 24 (2), 197–211.

Collins, D.L., Neelin, P., Peters, T.M., Evans, A.C., 1994. Automatic 3D intersubject registration of MR Volumetric data in standardized talairach space. J. Comput. Assist. Tomogr. 18 (2), 192–205.

Cosottini, M., Frosini, D., Pesaresi, I., Costagli, M., Biagi, L., Ceravolo, R., Bonuccelli, U., Tosetti, M., 2014. MR imaging of the substantia nigra at 7 T enables diagnosis of Parkinson Disease. Radiology 271 (3), 831–838.

Damier, P., Hirsch, E.C., Agid, Y., Graybiel, A.M., 1999a. The substantia nigra of the human brain I. Nigrosomes and the nigral matrix, a compartmental organization based on calbindin D28K immunohistochemistry. Brain 122, 1421–1436. https://doi. org/10.1093/brain/122.8.1421.

Damier, P., Hirsch, E.C., Agid, Y., Graybiel, A.M., 1999b. The substantia nigra of the human brain II. Patterns of loss of dopamine-containing neurons in Parkinson's disease. Brain 122, 1437–1448. https://doi.org/10.1093/brain/122.8.1437.

Draganski, B., Kherif, F., Kloppel, S., Cook, P.A., Alexander, D.C., Parker, G.J.M., Deichmann, R., Ashburner, J., Frackowiak, R.S.J., 2008. Evidence for segregated and integrative connectivity patterns in the human basal Ganglia. J. Neurosci. 28 (28), 7143–7152.

Du, A.-T., Schuff, N., Kramer, J.H., Rosen, H.J., Gorno-Tempini, M.L., Rankin, K., Miller, B.L., Weiner, M.W., 2006. Different regional patterns of cortical thinning in Alzheimer's disease and frontotemporal dementia. Brain 130, 1159–1166. https:// doi.org/10.1093/brain/awm016.

Folstein, M.F., Folstein, S.E., McHugh, P.R., 1975. Mini-mental state. J. Psychiatr. Res. 12 (3), 189–198.

Greicius, M.D., Srivastava, G., Reiss, A.L., Menon, V., 2004. Default-mode network activity distinguishes Alzheimer's disease from healthy aging: evidence from functional MRI. Proc. Natl. Acad. Sci. 101 (13), 4637–4642.

Hoehn, M.M., Yahr, M.D., 1967. Parkinsonism: onset, progression, and mortality. Neurology 17, 427–427. https://doi.org/10.1212/WNL.17.5.427.

Hughes, A.J., Daniel, S.E., Kilford, L., Lees, A.J., 1992. Accuracy of clinical diagnosis of idiopathic Parkinson's disease: a clinico-pathological study of 100 cases. J. Neurol. Neurosurg. Psychiatry 55 (3), 181–184.

Kabani, N., Le Goualher, G., MacDonald, D., Evans, A.C., 2001. Measurement of cortical thickness using an automated 3-D algorithm: a validation study. NeuroImage 13 (2), 375–380.

Kim, J.I., Sunwoo, M.K., Sohn, Y.H., Lee, P.H., Hong, J.Y., 2016. The MMSE and MoCA for screening cognitive impairment in less educated patients with Parkinson's disease. JMD 9 (3), 152–159.

Kim, J.S., Singh, V., Lee, J.K., Lerch, J., Ad-Dab'bagh, Y., MacDonald, D., Lee, J.M., Kim, S.I., Evans, A.C., 2005. Automated 3-D extraction and evaluation of the inner and outer cortical surfaces using a Laplacian map and partial volume effect classification. NeuroImage 27 (1), 210–221.

Kwon, D.-H., Kim, J.-M., Oh, S.-H., Jeong, H.-J., Park, S.-Y., Oh, E.-S., Chi, J.-G., Kim, Y.-B., Jeon, B.S., Cho, Z.-H., 2012. Seven-tesla magnetic resonance images of the substantia nigra in Parkinson disease. Ann. Neurol. 71 (2), 267–277.

Lee, J.S., Kim, C., Shin, J.-H., Cho, H., Shin, D.-S., Kim, N., Kim, H.J., Kim, Y., Lockhart, S.N., Na, D.L., Seo, S.W., Seong, J.-K., 2018. Machine learning-based individual assessment of cortical atrophy pattern in Alzheimer's disease spectrum: development of the classifier and longitudinal evaluation. Sci. Rep. 8 (1). https://doi.org/10.1038/ s41598-018-22277-x.

Lehéricy, S., Ducros, M., Van De Moortele, P.-F., Francois, C., Thivard, L., Poupon, C., Swindale, N., Ugurbil, K., Kim, D.-S., 2004. Diffusion tensor fiber tracking shows distinct corticostriatal circuits in humans: DTI corticostriatal fibers. Ann. Neurol. 55 (4), 522–529.

Lenglet, C., Abosch, A., Yacoub, E., De Martino, F., Sapiro, G., Harel, N., 2012. Comprehensive in vivo mapping of the human basal Ganglia and thalamic connectome in individuals using 7T MRI. PLoS One 7, e29153. https://doi.org/10.1371/ journal.pone.0029153.

Lerch, J.P., Evans, A.C., 2005. Cortical thickness analysis examined through power analysis and a population simulation. NeuroImage 24 (1), 163–173.

Mahlknecht, P., Krismer, F., Poewe, W., Seppi, K., 2017. Meta-analysis of dorsolateral nigral hyperintensity on magnetic resonance imaging as a marker for Parkinson's disease: DNH on MRI as a Marker for PD. Mov. Disord. 32 (4), 619–623.

Marquand, A.F., Haak, K.V., Beckmann, C.F., 2017. Functional corticostriatal connection topographies predict goal-directed behaviour in humans. Nat. Hum. Behav. 1 (8). https://doi.org/10.1038/s41562-017-0146.

Massey, L.A., Miranda, M.A., Al-Helli, O., Parkes, H.G., Thornton, J.S., So, P.-W., White, M.J., Mancini, L., Strand, C., Holton, J., Lees, A.J., Revesz, T., Yousry, T.A., 2017. 9.4 T MR microscopy of the substantia nigra with pathological validation in controls and disease. NeuroImage: Clin. 13, 154–163.

Mastaglia, F.L., Johnsen, R.D., Byrnes, M.L., Kakulas, B.A., 2003. Prevalence of amyloid-beta deposition in the cerebral cortex in Parkinson's disease. Mov. Disord. 18, 81–86. https://doi.org/10.1002/mds.10295.

McDonald, W.M., Holtzheimer, P.E., Haber, M., Vitek, J.L., McWhorter, K., DeLong, M., 2006. Validity of the 30-item geriatric depression scale in patients with Parkinson's disease. Mov. Disord. 21 (10), 1618–1622.

Mitchell, A.J., 2009. A meta-analysis of the accuracy of the mini-mental state examination in the detection of dementia and mild cognitive impairment. J. Psychiatr. Res. 43 (4), 411–431.

Nam, Y., Gho, S.-M., Kim, D.-H., Kim, E.Y., Lee, J., 2017. Imaging of nigrosome 1 in substantia nigra at 3T using multiecho susceptibility map-weighted imaging (SMWI): nigrosome 1 Imaging Using SMWI. J. Magn. Reson. Imaging 46 (2), 528–536.

Nandhagopal, R., Kuramoto, L., Schulzer, M., Mak, E., Cragg, J., Lee, C.S., McKenzie, J., McCormick, S., Samii, A., Troiano, A., Ruth, T.J., Sossi, V., de la Fuente-Fernandez, R., Calne, D.B., Stoessl, A.J., 2009. Longitudinal progression of sporadic Parkinson's disease: a multi-tracer positron emission tomography study. Brain 132 (11), 2970–2979.

Noh, Y., Sung, Y.H., Lee, J., Kim, E.Y., 2015. Nigrosome 1 detection at 3T MRI for the diagnosis of early-stage idiopathic parkinson disease: assessment of diagnostic accuracy and agreement on imaging asymmetry and clinical laterality. AJNR Am. J. Neuroradiol. 36 (11), 2010–2016.

Pereira, J.B., Svenningsson, P., Weintraub, D., Bronnick, K., Lebedev, A., Westman, E., Aarsland, D., 2014. Initial cognitive decline is associated with cortical thinning in early Parkinson disease. Neurology 82 (22), 2017–2025.

Schwarz, S.T., Afzal, M., Morgan, P.S., Bajaj, N., Gowland, P.A., Auer, D.P., 2014. The 'Swallow Tail' Appearance of the Healthy Nigrosome – A New Accurate Test of Parkinson's Disease: A Case-Control and Retrospective Cross-Sectional MRI Study at 3T. PLoS One. 9 (4), e93814. https://doi.org/10.1371/journal.pone.0093814.

Schwarz, S.T., Mougin, O., Xing, Y., Blazejewska, A., Bajaj, N., Auer, D.P., Gowland, P., 2018. Parkinson's disease related signal change in the nigrosomes 1–5 and the substantia nigra using T2* weighted 7T MRI. NeuroImage: Clin. 19, 683–689.

Shin, N.-Y., Hong, J., Choi, J.Y., Lee, S.-K., Lim, S.M., Yoon, U., 2017. Retrosplenial cortical thinning as a possible major contributor for cognitive impairment in HIV patients. Eur. Radiol. 27 (11), 4721–4729.

Shin, N.-Y., Shin, Y.S., Lee, P.H., Yoon, U., Han, S., Kim, D.J., Lee, S.-K., 2016. Different functional and microstructural changes depending on duration of mild cognitive impairment in Parkinson disease. Am. J. Neuroradiol. 37 (5), 897–903.

Sled, J.G., Zijdenbos, A.P., Evans, A.C., 1998. A nonparametric method for automatic correction of intensity nonuniformity in MRI data. IEEE Trans. Med. Imaging 17, 87–97. https://doi.org/10.1109/42.668698.

Sung, Y.H., Lee, J., Nam, Y., Shin, H.-G., Noh, Y., Shin, D.H., Kim, E.Y., 2018. Differential involvement of nigral subregions in idiopathic parkinson's disease: nigrosome 1 and 4 in Parkinson's disease. Hum. Brain Mapp. 39 (1), 542–553.

Sung, Y.H., Noh, Y., Lee, J., Kim, E.Y., 2016. Drug-induced Parkinsonism versus idiopathic Parkinson Disease: utility of nigrosome 1 with 3-T imaging. Radiology 279 (3), 849–858.

Uribe, C., Segura, B., Baggio, H.C., Abos, A., Garcia-Diaz, A.I., Campabadal, A., Marti, M.J., Valldeoriola, F., Compta, Y., Tolosa, E., Junque, C., 2018. Cortical atrophy patterns in early Parkinson's disease patients using hierarchical cluster analysis. Parkinsonism Related Disord. 50, 3–9.

Yau, Y., Zeighami, Y., Baker, T.E., Larcher, K., Vainik, U., Dadar, M., Fonov, V.S., Hagmann, P., Griffa, A., Mišić, B., Collins, D.L., Dagher, A., 2018. Network connectivity determines cortical thinning in early Parkinson's disease progression. Nat. Commun. 9 (1). https://doi.org/10.1038/s41467-017-02416-0.

Zarei, M., Ibarretxe-Bilbao, N., Compta, Y., Hough, M., Junque, C., Bargallo, N., Tolosa, E., Marti, M.J., 2013. Cortical thinning is associated with disease stages and dementia in Parkinson's disease. J. Neurol. Neurosurg. Psychiatry 84 (8), 875–882.

Zhou, G., Lane, G., Cooper, S.L., Kahnt, T., Zelano, C., 2019. Characterizing functional pathways of the human olfactory system. Elife 8, 1–27. https://doi.org/10.7554/ eLife.47177.

Zijdenbos, A.P., Forghani, R., Evans, A.C., 2002. Automatic "pipeline" analysis of 3-D MRI data for clinical trials: application to multiple sclerosis. IEEE Trans. Med. Imaging 21 (10), 1280–1291.